

X-ray structure of a cyclophilin B/cyclosporin complex: Comparison with cyclophilin A and delineation of its calcineurin-binding domain

(immunophilin/protein crystallography/immunosuppression)

VINCENT MIKOL, JÖRG KALLEN, AND MALCOLM D. WALKINSHAW

Preclinical Research, Sandoz AG, CH-4002 Basel, Switzerland

Communicated by Christopher T. Walsh, January 18, 1994

ABSTRACT The crystal structure of a complex between recombinant human cyclophilin B (CypB) and a cyclosporin A (CsA) analog has been determined and refined at 1.85-Å resolution to a crystallographic *R* factor of 16.0%. The overall structures of CypB and of cyclophilin A (CypA) are similar; however, significant differences occur in two loops and at the N and C termini. The CsA-binding pocket in CypB has the same structure as in CypA and cyclosporin shows a similar bound conformation and network of interactions in both CypB and CypA complexes. The network of the water-mediated contacts is also essentially conserved. The higher potency of the CypB/CsA complex versus CypA/CsA in inhibiting the Ca²⁺- and calmodulin-dependent protein phosphatase calcineurin is discussed in terms of the structural differences between the two complexes. The three residues Arg²⁰, Lys¹¹³, and Ala¹²⁸ and the loop containing Arg¹⁵⁸ on the surface of CypB are likely to modulate the differences in calcineurin inhibition between CypA and CypB.

Cyclophilins are conserved and ubiquitous proteins that bind cyclosporin A (CsA), which is the major drug used to prevent graft rejection after transplant surgery (1). Different classes of cyclophilins have been identified and shown to bind CsA and to possess peptidyl-prolyl cis-trans isomerase activity (2). The cyclophilin A (CypA) family (18 kDa), which is the most abundant, is localized in the nucleus and in the cytoplasm and is thought to be the intracellular target of CsA. The cyclophilin B (CypB) family (22 kDa) is distinguished from the CypA family by the presence of endoplasmic reticulum-directed signal sequences (3). NMR and x-ray structures of uncomplexed CypA (4), a tetrapeptide/CypA complex (5), and CsA/CypA complexes (6–9) have been reported. We present here the x-ray structure of the complex between recombinant mature CypB and a CsA analog.*

MATERIALS AND METHODS

Preparation of Crystals. CypB was purified (10) and concentrated to 20 mg/ml in 0.02% NaN₃. [D-Ser(choliny ester)⁸]CsA ([CES⁸]CsA) was synthesized by the method previously reported (11). Crystals of the CypB/[CES⁸]CsA complex were grown by vapor diffusion at 22°C by the hanging-drop method. The precipitating solution in the well consisted of 100 mM Tris-HCl (pH 8.0), 19.5% (wt/vol) PEG 8000, 5% (vol/vol) dimethyl sulfoxide, and 0.04% NaN₃. The initial 6-μl drop consisted of 50 mM Tris-HCl (pH 8.0), 9.75% (wt/vol) PEG 8000, 2.5% dimethyl sulfoxide, 0.02% NaN₃, 0.5 mM CypB, and 0.5 mM [CES⁸]CsA. This procedure yielded crystals within 3 weeks which often displayed intergrowth defects. Large single crystals could be obtained by seeding. A crystal was placed into a drop (15 μl) of reservoir

solution and washed twice with reservoir solution. It was then finely crushed and individual seeds (about 10 μm) were then transferred into drops of CypB/[CES⁸]CsA solution which had been equilibrated for 4 days against a reservoir solution of the same composition but slightly less concentrated in PEG 8000 [15% (wt/vol)]. The seeds grew to give well-formed orthorhombic crystals of about 0.5 mm × 0.4 mm × 0.3 mm within 2 weeks.

Data Collection and Processing. The x-ray intensity data were collected on a FAST area detector (Enraf Nonius, Delft, The Netherlands). Evaluation of the measured intensities was performed with the program MADNES (12). Refined cell dimensions are *a* = 37.40 Å, *b* = 46.86 Å, *c* = 115.40 Å, and the space group is *P*2₁2₁2₁. The crystal contains one complex per asymmetric unit and 53% solvent (*V*_M = 2.3 Å³/Da). A total of 56,456 reflections were measured which resulted in 15,219 unique reflections to a 1.85-Å *d* spacing (*R*_{sym} = 4.8% for 13,075 independent reflections). The completeness of the data up to 1.97 Å is 91% and is 52% for data between 1.97 and 1.85 Å. Data reduction was carried out with the CCP4 package (Daresbury Laboratory).

Structure Solution. The coordinates of the refined structure of the monomeric CypA/CsA complex (7) without CsA and water molecules were used as the model for phase determination by molecular replacement using XPLOR (13). Molecular building was carried out with the program o (14) and refinement was done with the XPLOR package (13). Plots were performed with the program MOLSCRIPT (15). The final model, which includes 196 solvent molecules, has been refined to an *R* factor of 16.0% with root-mean-square difference (rmsd) from target values for bond lengths and angles of 0.013 Å and 2.65°, respectively. The estimated error of the coordinates is about 0.17 Å as determined by a Luzzati plot. All non-glycine residues of CypB have φ and ψ angles which lie in allowed regions of the Ramachandran diagram. Alternative conformations for doubly disordered side chains of 12 residues could be determined.

RESULTS AND DISCUSSION

CypB Structure. The sequence of CypB is given in Fig. 1 and compared with that of CypA. Only two of the eight additional N-terminal residues could be located in the electron density. Sequencing of dissolved crystals has confirmed that six residues are missing at the N terminus, presumably cleaved off by proteases during the isolation of the protein. CypB displays the same folding as CypA (Fig. 2) but with

Abbreviations: CypA, cyclophilin A; CypB, cyclophilin B; CypC, cyclophilin C; CsA, cyclosporin A; [CES⁸]CsA, [D-Ser(choliny ester)⁸]CsA; MeBmt, (4*R*)-4-[(*E*)-2-butenyl]-4,*N*-dimethyl-L-threonine; rmsd, root-mean-square difference.

*The atomic coordinates have been deposited in the Protein Data Bank, Chemistry Department, Brookhaven National Laboratory, Upton, NY 11973. This information is embargoed for 1 year from the date of publication.

The publication costs of this article were defrayed in part by page charge payment. This article must therefore be hereby marked "advertisement" in accordance with 18 U.S.C. §1734 solely to indicate this fact.

	18	28	38	48	58
CypB	ADENKKGKVKIVKVFYDL	RIGDEEDVGRV	IFGLPGRVVE	KIVNEVALA	TQERGFQYRN
CypC	ALVFSSGAGGR.R.S.	AK.F.V	VI	V	E
CypA	M.NPT.F.I	AVDG.EL	S.E	ADK	AE.R.S
	10	20	30	40	50
	78	88	98	108	118
CypB	SEKFRVLDK	MIQGGDETAG	DGTGGKSIYG	ERFFDENFKL	KHYEGGVSM
CypCI.TVTIP
CypAI.PGCH.NK.EI
	60	70	80	90	100
	138	148	158	169	179
CypB	WLDGRVVFVFG	KVLEGGMEVVR	KVESTKIDSR	DRFLDVLID	OGKIEVEKPF
CypCIDT.HSI.LQAGER
CypAKN.I.EAM.RFGSRNGTS.KITGL
	130	140	150	160	

FIG. 1. Sequence alignment of CypB, CypC, and CypA. Dots indicate residues identical to those in CypB and stars represent residues which are within 4.0 Å of CsA. CypA (165 residues) has 64% overall sequence identity with CypB (184 residues) (75% in the central part of the molecule—i.e., between residues 41–136 of CypA and residues 49–144 of CypB). CypC (194 residues) has 70% sequence identity with CypB. The crystal structure described here is for residues 7–184 of CypB.

differences in two loops (residues 19–24 and 152–164 of CypB) and in the extensions at the N and C termini.

In CypA, the N terminus was characterized by an extended β -strand (residues 1–11). In CypB, this β -strand (residues 12–19) bends at residue 12 toward the barrel and the first three residues, nos. 7–9, start a new β -strand. The additional 10 amino acids at the C terminus of CypB (Val¹⁷⁵–Glu¹⁸⁴) extend the last β -strand and then make a type VIII β -turn and start a new strand (Fig. 2). Both extensions at the N and C termini lie far away from the CsA binding site.

The loop connecting the two first β -strands in CypA (Val¹²–Asp¹³–Gly¹⁴–Glu¹⁵) corresponds to a β -hairpin with a type I' β -turn structure. In CypB (Ile²⁰–Gly²¹–Asp²²–Glu²³), this turn has twisted to give a slightly distorted type II' β -turn, as is relatively commonly found when glycine occurs in position ($i+1$) of a β -turn (16). This loop is canted at a different angle in CypA than in CypB, probably because of hydrogen bonds between side chains of the loop and the rest of the molecule.

The 11-amino acid loop connecting the second α -helix to the next β -strand in CypB (residues Thr¹⁵³–Lys¹⁶³) adopts a very different conformation than the corresponding 10-amino acid loop (Phe¹⁴⁵–Lys¹⁵⁴) in CypA (Fig. 3). There is no sequence homology between residues in the two loops and the rmsd between the backbone atoms of the nine corresponding residues is 3.5 Å.

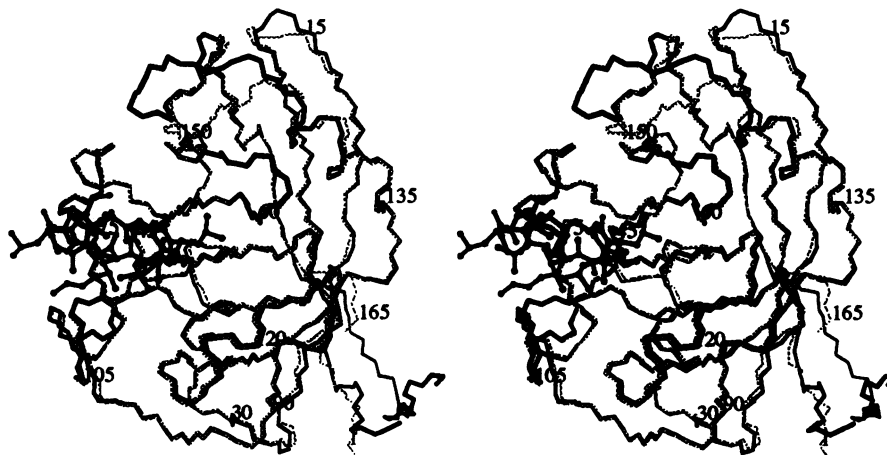


FIG. 2. Comparison between CypA and CypB. Superposition of the backbone trace of CypB (black) on that of CypA (gray). Some residues of CypA are labeled. The rmsd between residues 1–143 of CypA and residues 9–151 of CypB is 1.02 Å for backbone atoms. The part of the new β -strand made by residues 7–9 of CypB is hydrogen-bonded with some backbone atoms of the β -strand made by residues 23–32 and to the C-terminal extension. Then the residues Val¹² and Thr¹¹ of CypB induce a 90° bend of this β -strand.

The CsA Molecule. The refined x-ray structure of CsA bound to CypA indicated that all peptide bonds of CsA are in the trans configuration and revealed the existence of an intramolecular hydrogen bond between the hydroxyl group of the (4*R*)-4[(*E*)-2-butenyl]-4,*N*-dimethyl-L-threonine residue (MeBmt¹) and the carbonyl oxygen atom of MeLeu⁴ (6, 7). This is also observed in the present complex. A superposition of CypA-bound CsA on CypB-bound [CES⁸]CsA using only the backbone atoms gives an rmsd of 0.23 Å, indicating that the conformation of the peptide ring has remained unchanged. The only significant structural difference is the orientation of the side chain of MeLeu⁴, where χ^1 and χ^2 angles have changed from -108° and -50° in the CypA/CsA complex to -58° and -167° in the CypB/[CES⁸]CsA complex. This is close to the most frequently observed (50%) rotamer of leucine (gauche⁺, trans) (17). The cholanyl ester derivatization in position 8 could not be detected in the electron density map, probably because of high flexibility. Five water molecules are hydrogen-bonded to [CES⁸]CsA (distance cutoff, 3.2 Å) through the carbonyl oxygen atoms of MeBmt¹, sarcosine-3 (Sar³), MeLeu⁶, and Ala⁷ and through the nitrogen atoms of Val⁵ and of CES⁸. Four of these were also found in the CsA/CypA complex (7).

The Binding Pocket. The direct hydrogen-bonding pattern (five direct hydrogen bonds) is similar to the interactions found in the CypA/CsA complex. There are no differences in sequence or structure (rmsd < 0.15 Å) between the two complexes for any residues of the binding pocket within 5.0 Å of CsA, as previously suggested by an NMR study (18). Four solvent molecules mediate interaction between [CES⁸]CsA and CypB. The water-mediated contacts are also essentially conserved. Despite the similarity of the active site, the inhibition of the peptidyl-proline cis-trans isomerase activity by CsA is slightly different for CypA (IC₅₀ = 25 nM) and CypB (IC₅₀ = 84 nM) (3).

Calcineurin Inhibition. The protein-serine/threonine phosphatase activity of calcineurin is inhibited by the complex of cyclophilin with CsA, though neither cyclophilin alone nor CsA alone shows any inhibition (19). The CypB/CsA complex is 14-fold more effective (K_i < 21 nM) than the CypA/CsA complex (K_i = 336 nM) in inhibiting calcineurin (20), whereas CypC/CsA is slightly less active than CypA/CsA in inhibiting calcineurin (M. Zurini, personal communication). The protruding effector region of CypA-bound CsA, comprising MeLeu⁴, Val⁵, and MeLeu⁶, has been shown to be crucial for the interaction and inhibition of calcineurin (21). [CES⁸]CsA bound to CypB adopts a backbone conformation

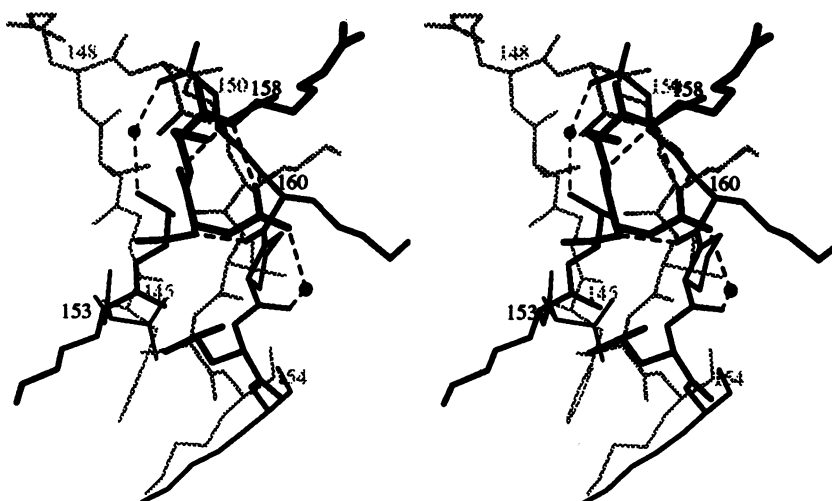


FIG. 3. Comparison of the loop containing Arg¹⁴⁸ in CypA (gray) and Arg¹⁵⁸ in CypB (black). This long U-shaped loop in CypB, which makes a type I β -turn, contains intramolecular hydrogen bonds between side chains and backbone atoms. They maintain the overall conformation of the loop. Two water-mediated contacts further rigidify the loop (average temperature factor of the atoms of the loop is 17.2 \AA^2 , compared with 15.1 \AA^2 for the whole molecule).

almost identical to that found in the CypA/CsA complex, and differences in calcineurin inhibition between CypA/CsA and CypB/CsA are likely, therefore, to be due to differences in cyclophilin residues. Amino acids on CypB which are potentially responsible for the enhanced inhibition are listed in Table 1. They comprise those solvent-exposed residues of CypA, -B, and -C which differ in sequence and lie within 16 \AA from the effector loop of CsA. Site-directed mutation of Arg¹⁴⁸ to Glu in CypA (R148ECypA mutant) resulted in a 20-fold improved inhibition of calcineurin by the R148ECypA/CsA complex when compared with CypA/CsA, whereas the neutral change Arg¹⁴⁸ to Leu had no significant effect. These results led to the suggestion that position 148 in CypA is an important contact site for calcineurin (20). However, the large differences in sequence and conformation between CypA and CypB in this

loop (Fig. 3) make it difficult to estimate the importance of individual side chains in the interaction with calcineurin. In addition to this loop, the analysis of the solvent-exposed residues summarized in Table 1 highlights three residues of CypB—namely Arg⁹⁰, Lys¹¹³, and Ala¹²⁸—which are different in CypA, CypB, and CypC. Any or all of these residues may also be responsible for the enhanced effectiveness of CypB. Fig. 4 shows the CypA surface around CsA and differences with CypB. The surface of CypA within 8 \AA of the effector domain of CsA, along with the effector surface of CsA, probably defines a conserved calcineurin-binding area. The three residues and the Arg¹⁵⁸ loop of CypB identified in Table 1 lie on the edge of this region and are therefore likely to modulate the differences in calcineurin binding among the cyclophilin family. This hypothesis can be tested by site-directed mutagenesis.

Table 1. Solvent-exposed residues which differ between CypA and CypB

Residues			Distance from the effector side of CsA, \AA		Accessible surface area, \AA^2	
CypA	CypB	CypC	CypA	CypB	CypA	CypB
C52	K60	K	15.4	15.6	8	44
P58	K66	K	15.1	15.3	64	110
G59	D67	D	16.4	16.0	53	98
H70	G78	G	13.1	13.1	79	17
N71	D79	D	8.5	8.5	82	89
K82	R90	T	11.7	6.5	120	78
P105	K113	P	13.1	10.6	106	165
E120	A128	T	11.3	16.5	84	53
G146	K154	A	15.7	18.2	19	152
S147	T155	T	13.5	14.8	28	51
R148	D156	D	10.7	12.9	210	58
N149	S157	G	8.7	11.0	99	115
G150	R158	H	10.1	7.9	1	198
K151	D159	D	10.6	8.9	152	50
T152	K160	R	14.6	11.8	44	66
S153	P161	P	17.8	14.3	92	5

Amino acid residues (single-letter symbols) of CypA and CypB were selected if they lay within 16 \AA of the C α atoms of MeLeu⁴ or of Val⁵ or of MeLeu⁶ (the effector domain of CsA). Corresponding residues for CypC are also shown. Residues which are different in CypA, CypB, and CypC are in bold type. The accessible surface areas were computed with the program AREAIMOL (CCP4, Daresbury Laboratory) after removal of the crystallographic water molecules.

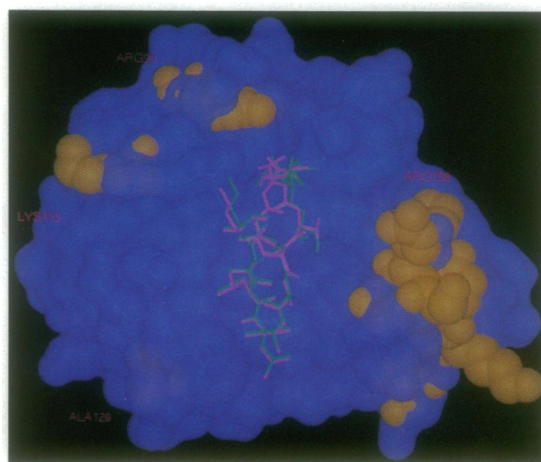


FIG. 4. Surface of the CypA/CsA complex and comparison with CypB/[CES^B]CsA. CypB was superimposed on CypA by using the first 143 C α atoms of CypA. The blue slightly transparent surface corresponds to the CypA surface. The CypA atoms are displayed in cyan under the surface. The CypA-bound CsA and the CypB-bound [CES^B]CsA are shown in green and pink, respectively. The three residues (Arg⁹⁰, Lys¹¹³, and Ala¹²⁸) and the Arg¹⁵⁸ loop, which differ in sequence among CypA, -B, and -C (see Table 1), are displayed with a yellow Corey-Pauling-Koltun model. Ala¹²⁸ cannot be seen easily, as it sits behind the CypA surface. The picture was made by using the program VIEW written by M. Sanner.

We thank J. Causevic and M. Zurini for the purification of recombinant human CypB, D. Duc for help in crystallization, and P. Graff for amino acid sequence analysis of dissolved crystals.

1. Borel, J.-F. (1989) *Pharmacol. Rev.* **41**, 259–371.
2. Galat, A. (1993) *Eur. J. Biochem.* **216**, 689–707.
3. Price, E. R., Zydowsky, L. D., Jin, M., Baker, C. H., McKeon, F. D. & Walsh, C. T. (1991) *Proc. Natl. Acad. Sci. USA* **88**, 1903–1907.
4. Ke, H., Zydowsky, L. D., Liu, J. & Walsh, C. T. (1991) *Proc. Natl. Acad. Sci. USA* **88**, 9483–9487.
5. Kallen, J., Spitzfaden, C., Zurini, M. G. M., Wider, G., Widmer, H., Wüthrich, K. & Walkinshaw, M. D. (1991) *Nature (London)* **353**, 276–279.
6. Pflügl, G., Kallen, J., Schirmer, T., Jansonius, J. N. & Walkinshaw, M. D. (1993) *Nature (London)* **361**, 91–94.
7. Mikol, V., Kallen, J., Pflügl, G. & Walkinshaw, M. D. (1993) *J. Mol. Biol.* **234**, 1119–1130.
8. Thériault, Y., Logan, T. M., Meadows, R., Yu, L., Olejniczak, E. T., Holzman, T. F., Simmer, R. L. & Fesik, S. W. (1993) *Nature (London)* **361**, 88–91.
9. Spitzfaden, C., Weber, H.-P., Braun, W., Kallen, J., Wider, G., Widmer, H., Walkinshaw, M. D. & Wüthrich, K. (1992) *FEBS Lett.* **300**, 291–300.
10. Spik, G., Haendler, B., Delmas, O., Mariller, C., Chamoux, M., Maes, P., Tartar, A., Montreuil, J., Stedman, K., Kocher, H. P., Keller, R., Hiestand, P. C. & Movva, R. (1991) *J. Biol. Chem.* **266**, 10735–10738.
11. Wenger, R. (1984) *Helv. Chim. Acta* **67**, 502–525.
12. Messerschmidt, A. & Pflugrath, J. W. (1987) *J. Appl. Crystallogr.* **20**, 306–315.
13. Brünger, A. T. (1992) *x-PLOR Manual* (Yale Univ. Press, New Haven, CT), Version 3.1.
14. Jones, A. T., Zou, J.-Y., Cowan, S. W. & Kjeldgaard, M. (1991) *Acta Crystallogr.* **A47**, 110–119.
15. Kraulis, P. J. (1991) *J. Appl. Crystallogr.* **24**, 946–950.
16. Wilmot, C. J. & Thornton, J. M. (1988) *J. Mol. Biol.* **203**, 221–232.
17. Schrauber, H., Eisenhaber, F. & Argos, P. (1993) *J. Mol. Biol.* **230**, 592–612.
18. Neri, P., Gemmecker, G., Zydowsky, L. D., Walsh, C. T. & Fesik, S. W. (1991) *FEBS Lett.* **290**, 195–199.
19. Liu, J., Farmer, J. D., Lane, W. S., Friedman, J., Weissman, I. & Schreiber, S. L. (1991) *Cell* **66**, 807–815.
20. Etzkorn, F. A., Chang, Z., Stolz, L. A. & Walsh, C. T. (1994) *Biochemistry* **33**, 2380–2388.
21. Schreiber, S. L. (1992) *Cell* **70**, 365–368.